CrossMark

ORIGINAL PAPER

Electrochemical deposition of silica sol–gel films on stainless steel: preliminary analysis of key variables

Gianmarco Giordano[1] · Christian Durante[2] · Armando Gennaro[2] · Massimo Guglielmi[1]

Abstract The sol–gel electrodeposition of coatings on conductive substrates has been presented the first time in 1999, and since then, a significant number of papers have been published, mainly devoted to explore the possibilities of application. However, a clear and complete picture of the fundamental aspects and of the role of the many parameters involved is still lacking. In this work, which is intended to be a preliminary approach to a systematic study, the effect of potential and time on the coating thickness was studied, trying to analyze the different factors that make experimentation difficult, looking for possible solutions and putting the basis for a more complete and analytic investigation. Simple tetraethyl orthosilicate-based acidic solutions were used to coat planar stainless steel samples. Different starting solutions were tested, varying the amount of precursor, water and hydrochloric acid. The role of working temperature, oxygen concentration and the presence of potassium nitrate until saturation was tested. Morphology, thickness, cyclic voltammetry and chronoamperometry were used to characterize the coatings and to monitor the current in function of potential and time. The thickness was found to increase with both the concentration of the solution and the HCl/TEOS ratio. Temperature was found to be an important factor, but also the amount of oxygen and electrolyte (KNO_3) in solution seems to influence the thickness of coatings.

Graphical Abstract
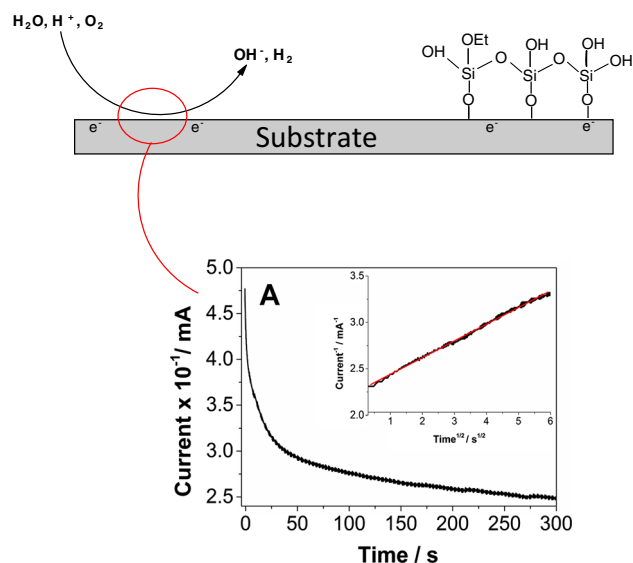
1 Introduction

The formation of thin films on various type of substrates is among the most important and successful technological applications of the sol–gel process. Dip coating, spin coating and spray coating are the principal coating methods. Each of them has, of course, advantages and disadvantages, but a common problem they have is that it is difficult to coat objects with complex or hidden surfaces, at least in a controlled way.

✉ Massimo Guglielmi
   massimo.guglielmi@unipd.it

[1] Dipartmento di Ingegneria Industriale, Università di Padova, Via Marzolo 9, 35135 Padua, Italy

[2] Dipartmento di Scienze Chimiche, Università di Padova, Via Marzolo 1, 35131 Padua, Italy

Springer

In 1999, Shacham et al. [1] developed a new deposition method that might, in principle, solve this problem for electrical conductive surfaces. It is based on the local electrochemical generation of catalysts (hydroxide ions or protons) to increase the rate of sol–gel reactions. In the case of basic catalysis, and following the idea of the two-step method, the hydrolysis is carried out initially in acidic medium and the polycondensation is favored at the solution–substrate interface by a local increase in pH induced by the application of a sufficiently negative constant potential, which promotes the reduction reactions of oxygen and water. The same authors published two articles in which they showed that it is possible to deposit zirconia [2] and titania [3] films. Since then, the electro-assisted deposition has been used to produce nanocomposites [4–6], anticorrosion protective layers [7–16] and mesoporous silica [17–20]. More recently, an interesting application of the mechanism of electrodeposition has been exploited: the formation of patterns using the scanning electrochemical microscopy (SECM) to locally increase the electron concentration and therefore the electro-generation of hydroxide ions [21].

The cited literature reports on the influence of the most important parameters (potential, time, concentration of precursors, stirring, electrolyte) on the properties of the deposited layers (thickness, morphology, resistance to corrosion), and some of the studies are very well detailed with important key information. However, they are often made using different experimental methods and systems that cannot be easily compared. Therefore, a clear picture of the fundamental aspects and of the real role played by the many parameters involved is still lacking, and many questions need for an answer, which is preliminary for the full development and application of this coating method.

This paper is a first attempt to get a broader understanding of the key parameters and of their influence on the obtained coatings.

The fundamentals of electrochemical deposition method involve many different theoretical aspects, and the practical results of the application of the method are the sum of many contributions. Therefore, it is not easy to perform experiments taking everything into account or deciding what is most important.

In this work, which is intended to be a preliminary approach to a systematic study, the effect of potential and time on the thickness was studied using simple TEOS-based (TEOS = tetraethyl orthosilicate) acidic solutions to coat planar stainless steel samples. Different starting solutions were tested, varying the amount of precursor, water and hydrochloric acid. The role of working temperature, oxygen concentration and the presence of KNO_3 until saturation was also tested.

2 Experimental

The starting solutions were prepared by mixing, in the following order, ethanol, distilled water, hydrochloric acid and tetraethyl orthosilicate (TEOS) as precursor for silica. Different batches were obtained changing the following parameters: $C = SiO_2$ g/L (from 50 to 150), $R = H_2O/TEOS$ molar ratio (from 2 to 10) and $H = HCl/TEOS$ molar ratio (from 0.005 to 0.02). The solutions were pre-hydrolyzed for 1 h at room temperature while stirring.

TEOS (98%) and ethanol ($\geq$99.8%) were purchased from Sigma-Aldrich and used as received. Hydrochloric acid (1 M) was used.

The electrodeposition was obtained by using a potentiostat/galvanostat (EG&G PARC, Model 273A) within a standard three-electrode cell. The reference electrode was a saturated calomel electrode (SCE), and the counter electrode was a platinum wire. The working electrodes were obtained from a stainless steel sheet (AISI 304), protected on one side by a protective removable film. The surface was mirror-like polished, and the roughness was the same for all samples. The dimensions of the plates were $20 \times 10 \times 1$ mm^3. When carrying out cyclic voltammetry, an exposed area of approximately 7 mm^2 was obtained with the help of adhesive Teflon. Teflon has also been used to mask the edges of the samples during the depositions and left an exposed circular area of about 40 mm^2. In order to control the process temperature, an external thermostat was used, which was connected to the water jacket of the cell. No stirring was applied during the deposition. After application of the potential, the samples were withdrawn by a dip coater with a withdrawal constant rate of ca. 100 μm/s.

It must be underlined that, during extraction from the batch, a layer is deposited by "dip coating" on the electrochemically deposited layer. This can be reduced by using a very low withdrawal rate, but cannot be avoided. Therefore, the final coating is made of two layers, different in thickness and presumably different in density, degree of condensation, *etc*. This makes the analysis of the results more complicated. Some authors rinsed [22] or blow-dried (with nitrogen [10]) the samples after deposition, assuming that the layer deposited by dipping could be removed leaving the electrodeposited layer mostly unaffected. Here, it was decided to measure the thickness of the dipping layer by depositing it using the same solutions, but without any voltage applied, and to take this thickness into account when evaluating the electrodeposited one, by subtracting the first from the total thickness measured.

The samples were dried at room temperature for at least 24 h before each characterization.

The surface morphology and the composition of the films were investigated in low vacuum by scanning electron

microscopy and energy dispersive X-ray analysis (SEM/EDX, Philips XL30), while the thickness was measured by a variable-angle spectroscopic ellipsometer (VASE) at incident angles of 70°, 75° and 80°, within a wavelength range of 300–1700 nm. The thickness was fitted using a Cauchy model. For each kind of solution, a cyclic voltammetry (CV) was performed with different switching potential and chronoamperometric (CA) data were acquired during the deposition runs.
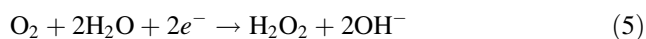
3 Results and discussion

3.1 General concepts

The application of a constant negative potential gives rise to the increase in pH at the electrode surfaces, due to reduction reactions of oxygen and water, which in acidic environment involve the consumption of protons:

$$O_2 + 4H^+ + 4e^- \rightarrow 2H_2O \tag{1}$$

$$2H^+ + 2e^- \rightarrow H_2 \tag{2}$$
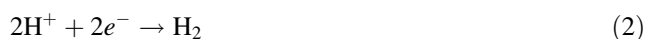
reaching neutral or basic medium, where the production of hydroxide ions takes place:

$$O_2 + 2H_2O + 4e^- \rightarrow 4OH^- \tag{3}$$

$$2H_2O + 2e^- \rightarrow H_2 + 2OH^- \tag{4}$$

$$O_2 + 2H_2O + 2e^- \rightarrow H_2O_2 + 2OH^- \tag{5}$$

Depending on the initial acidity, the solution may become basic, promoting hydrolysis and condensation under this regime, with all known consequences on the network formation. Initially, this situation is confined close to the sample surface, but immediately, due to the concentration gradient (diffusion) and the electric field (migration), unreacted hydroxyl ions move away from the surface region generating a complex pH gradient in the solution. If the batch is mechanically stirred, the situation becomes even more complex, with the addition of a convective term. The increase in the pH in the solution changes the kinetics of the reactions involved in the sol-to-gel transition. How all these phenomena affect the layer deposited on the sample surface (thickness, morphology, density, etc.) is hard to predict, and the experimental approach seems the most convenient one, taking the general picture as a base for a (at least qualitative) interpretation of the results.

3.2 Influence of sample shape

A first aspect that has to be taken into account when measuring the thickness of the electrodeposited layer is related to the shape of the sample. It is known from the electroplating practice that the deposited layers are thicker at sharp corners and edges and thinner in recessed areas due to the inhomogeneous distribution of the electric field. In the case of electrochemical sol–gel deposition for the same reason the reduction reactions should not occur homogeneously on the surface, generating a strong pH gradient and, as a consequence, a variation of the thickness from the edge to the center of the sample.

To estimate this effect, a stainless steel sample was coated using a solution characterized by $C = 50$, $R = 6$ and $H = 0.01$, at -0.7 V for 5 min at 27 °C. Figure 1 shows the ESEM (environmental scanning electron microscopy) image of the layer at the edge where the thickness is about 5 μm. The thickness was also measured at the center of the sample and in between the edge and the center by ellipsometry, obtaining values of 90 and 120 nm, respectively.

Based on this observation, all the samples used for this study were masked at the edges with a Teflon tape, leaving an exposed area of about 40 mm^2, to minimize the edge effect.

The thicknesses were measured in the central area of the coated samples, which were sufficiently homogeneous, as can be seen from a typical ESEM image reported in Fig. 2.

3.3 Influence of potential and time

With the help of cyclic voltammetry and using a blank solution with ethanol instead of TEOS, it was found that the reduction in water begins at -0.7 V versus SCE. Therefore, for the electrodeposition in the presence of TEOS, three different potentials were applied for 2 min
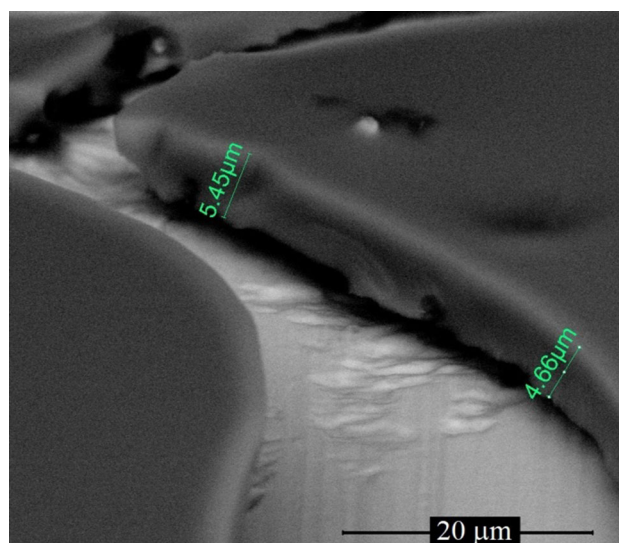

Fig. 1 ESEM image of SiO$_2$ film deposited at -0.7 V versus SCE for 5 min at 27 °C. Detail of the edge
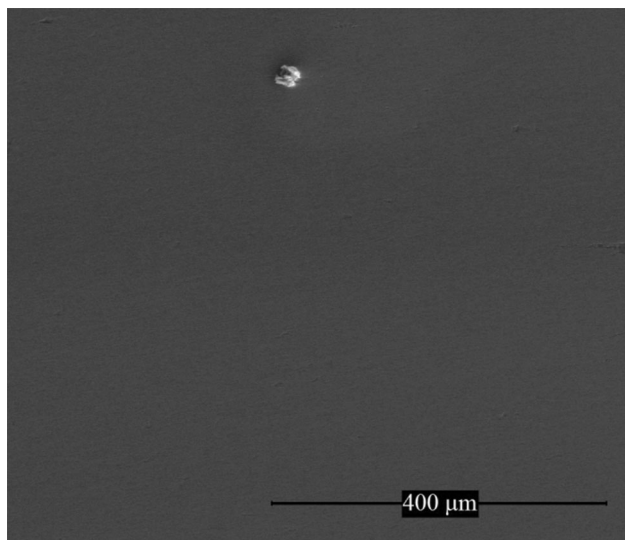
Fig. 2 ESEM micrographs of SiO$_2$ films deposited at −0.7 V versus SCE for 2 min at 27 °C
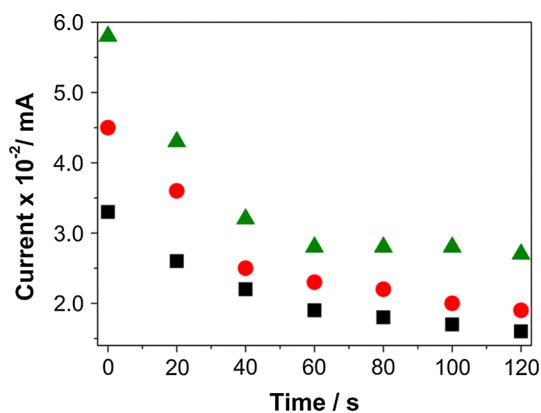

Fig. 3 Chronoamperometric data. Deposition time: 2 min. Applied potentials: −0.7 V (*square*), −0.9 V (*circle*), −1.1 V (*triangle*)

(−0.7, −0.9 and −1.1 V versus SCE), keeping constant the temperature and the solution ($C = 50$, $R = 6$ and $H = 0.01$).

A chronoamperometry was acquired for each sample during the deposition (Fig. 3). As expected, the initial

current increases with the absolute value of the applied potential.

The thickness was measured by ellipsometry in the central area of the samples, as explained above. The mean value of the thickness and the optical constants were obtained by applying the Cauchy model. Table 1 reports the thickness of the electrodeposited layers. As already observed, the final coating is made of a first layer deposited electrochemically and a second one due to the withdrawal process after the electrodeposition. To take into account this last contribution to the total thickness, a silica film was deposited by simple dipping without any applied potential. A thickness of 53.9 ± 1.0 nm was measured, which, subtracted to the total thickness, gives the estimated thickness of the electrodeposited layer.

As reported in the literature, the thickness increases with the absolute value of the applied potential [1]. It increases also with time, but different trends are reported. Data published by Shacham et al. on TiO$_2$ and ZrO$_2$ coatings indicate that a constant thickness regime is reached after 10–15 min, but in a paper recently published by Farghaly et al. [6] the thickness of silica-based nanocomposite films increases almost linearly with time up to the maximum tested period of 30 min. Our measurements show a linear increase up to 120 min.

3.4 Influence of the solution composition

The thickness of the deposited layers was studied as a function of the concentration of precursor, water and hydrochloric acid. The potential and deposition time were fixed at −0.9 V versus SCE and 5 min, respectively.

In order to avoid trivial errors, DOE (design of experiments) was used to plan the experiments. Three factors were considered (C, R, H) with two levels each: low and high concentration (Table 2). Therefore, the full factorial design requires eight experiments, which are denoted with minuscule letters following the Yates's notation [23]. Experiments denoted with a single letter are aimed to test the influence of a single parameter, while experiments denoted with two or three letters are aimed to test the interaction between two or among three parameters. The

Table 1 Thickness of silica films measured by ellipsometry in the central area of the samples

Sample	Potential (V versus SCE)	Time (min)	Thickness (nm)	Estimated electrodeposited thickness (nm)
p1	−0.7	2	125.3 ± 1.8	71 ± 3
p2	−0.9	2	121.3 ± 3.6	67 ± 4
p3	−1.1	2	196.5 ± 4.3	143 ± 5
t1	−0.9	30	181 ± 18	127 ± 18
t2	−0.9	120	338 ± 5	284 ± 6

Table 2 Factors and levels in DOE

Factor	Low	High
C	100	150
R	2	10
H	0.005	0.02

corresponding solution formulations are reported in Table 3.

Before the deposition, a cyclic voltammetry curve was obtained for each solution. For the determination of the reduction potential of hydrogen, it was assumed that TEOS behaves as ethanol, and solutions c, r and h (where TEOS was replaced with the appropriate amount of ethanol) were used. The results are shown in Fig. 4.

By increasing the concentration of water and HCl, the current increases, but the potential at which hydrogen reduces remains constant.

During the deposition, the potentiostat provides the current as a function of time (chronoamperometry, CA). The current depends on the nature of the solution, but also on the thickness of the silica layer that is forming, on the size, amount and morphology of the pores. To the best of our knowledge, these aspects were not studied thoroughly, although they are important both from the point of view of the understanding of the process and of the practical application. At the beginning, current always decreases, according to the trend of Fig. 3, but after this decrease, two different behaviors were observed:

- Experiments that had a factor H with a low level (0.005) followed the same trend as shown in Fig. 5a, with a continuous decrease of current with time;
- experiments that had a factor H with a high level (0.02) showed a trend similar to the one reported in Fig. 5b, with an increase in the current after about 20 s until to reach a constant value.

According to Shacham et al. [2], a linear dependence can be observed by plotting i^{-1} as a function of $t^{1/2}$, at least in the first period of the deposition (Fig. 5, insets). This behavior can be explained assuming diffusion-controlled
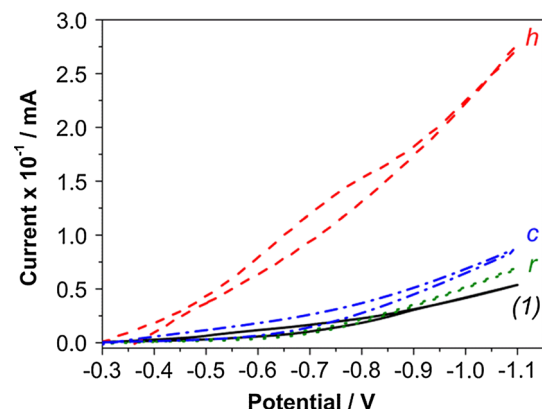

Fig. 4 Cyclic voltammetry. Scan rate 200 mV/s. Switching potential: −1.1 V versus SCE

conditions following the Cottrell equation for semi-infinite diffusion [24, 25]

$$i(t) = \frac{nFACD^{1/2}}{(\pi t)^{1/2}}$$

which is valid only for short time period, while the deviation from linearity for long periods is due to the finite nature of the film.

The trend shown in Fig. 5b has been observed in the electrochemical deposition of metals and has been discussed in terms of three contributions: adsorption, 2D nucleation and growth, 3D nucleation with diffusion-controlled growth [26]. The mechanism of film deposition in the case described here is, of course, different, and the observed trend cannot be explained in the same way, even if some analogy might be found. A specific study is necessary to relate, for example, the shape of the current–time curves with the morphology of the deposited layers.

After deposition, the samples were withdrawn from the solution and dried, as already described in the experimental section. After few seconds, the samples r, cr, rh and crh cracked on the whole surface (Fig. 6b), while the samples with a low water content ($R = 2$, corresponding to the treatments (1), c, h, ch) were free of cracks, at least in a wide central area (Fig. 6a). It was, of course, impossible to

Table 3 Tested solutions

Solution	Ethanol (mL)	H$_2$O (mL)	HCl (1 M) (mL)	TEOS (mL)
(1)	28.7	2.6	0.4	18.3
c	18.1	3.8	0.6	27.5
r	16.9	14.4	0.4	18.3
cr	0.4	21.5	0.6	27.5
h	28.7	1.36	1.64	18.3
ch	18.1	1.94	2.46	27.5
rh	16.9	13.16	1.64	18.3
crh	0.4	19.64	2.46	27.5

Fig. 5 Chronoamperometric data. Deposition time: 5 min. Applied potential: −0.9 V versus SCE. Sample cr on the left and sample rh on the right
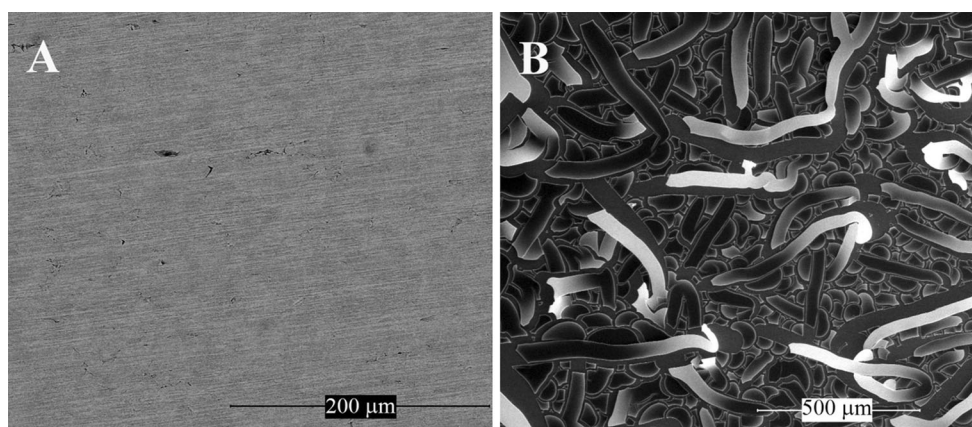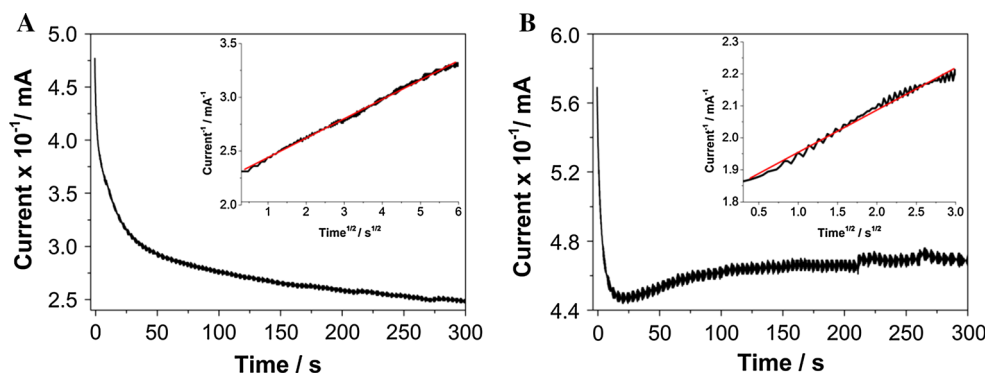

Fig. 6 ESEM micrographs. **a** Sample (1) deposited at −0.9 V versus SCE for 5 min. **b** Sample cr deposited at −0.9 V versus SCE for 5 min

Table 4 Composition and ellipsometric thickness data of samples used to evaluate the influence of the solution composition

Samples	C	R	H	Thickness (nm)	Dipping thickness (nm)	Estimated electrodeposited thickness (nm)
(1)	100	2	0.005	300 ± 14	149.0 ± 1.5	151 ± 14
c	150	2	0.005	580 ± 16	232.9 ± 3.5	347 ± 16
h	100	2	0.02	449 ± 9	139.9 ± 2.5	309 ± 9
ch	150	2	0.02	586 ± 26	204.0 ± 1.9	382 ± 26

get thickness data from ellipsometry in the first four samples, due to scattering. The thickness of the other samples is reported in Table 4. Also in this case, layers at null voltage were produced to get the "dipping" thickness and estimate the electrochemical thickness.

It is interesting to compare the "dipping" thickness and the estimated electrodeposited thickness. The "dipping" thickness clearly increases, as known, with precursor concentration, but it seems to slightly decrease with acid concentration. This might be related to the structure of the hydrolyzed species and to the related viscosity of the sol. Considering the estimated electrochemical thickness, it increases with precursor concentration, according to Okner et al. [27]. It also increases with the factor H, i.e., with the acidity of the solution. One might argue that starting from a

lower initial pH should minimize the local increase in pH due to protons consumption at the sample surface, thus decreasing the layer growth and consequently the thickness at a given deposition time. However, at lower pH, the hydrolysis rate of the precursor increases. More hydrolyzed species should be therefore available in the solution, prompt to condense at the sample surface. The higher thickness measured when both C and H are high seems to confirm this tentative explanation.

3.5 Influence of temperature, oxygen and electrolyte

The temperature is an important variable, because it affects the kinetics of diffusion and promotes Ostwald ripening, changing the morphology of the film [28]. The concentration

Table 5 Thickness, measured by ellipsometry, of layers deposited at $T = 41\ ^\circ\text{C}$

Sample	Thickness (nm)	Estimated electrodeposited thickness (nm)
T	173.4 ± 2.6	120 ± 3
oT	241.2 ± 2.4	187 ± 3
eT	222.2 ± 1.6	168 ± 2

of oxygen in solution might also be important, as it affects reactions (1), (3) and (5). The electrolyte is usually considered as not directly participating in the electron transfer reaction. However, as pointed out by Collinson et al. [29], the electrolyte's chemical properties can enable direct reactions at the electrode surface or reactions with species electro-generated at an electrode surface. Potassium nitrate was indeed used by Ding et al. [30] to promote OH⁻ production by the reaction

$$NO_3^- + H_2O + 2e^- \rightarrow NO_2^- + 2OH^-$$
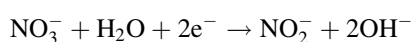
Therefore, these three further parameters were tested.

The starting solution used for these experiments had $C = 50$, $R = 6$ and $H = 0.01$. A potential of -0.9 V versus SCE was applied for 5 min. Three experiments were run: at 41 °C in the absence of oxygen and KNO_3 in solution (T), at 41 °C in the presence of oxygen in solution (oT) and at 41 °C in the presence of KNO_3 in solution (eT). The oxygen saturation was ensured by bubbling O_2 into the solution in the cell for 20 min and blowing O_2 above the solution during the whole deposition, whereas the absence of oxygen was guaranteed by bubbling argon into the solution for 20 min before the deposition. For the experiment eT, the solution was saturated with KNO_3.

All the samples were qualitatively better (more homogeneous, crack free) than those obtained at room temperature, suggesting that the process temperature may be an important factor for obtaining good quality layers. However, a more systematic study is needed to better support this finding.

The thickness of the coatings deposited in the three experiments is reported in Table 5. A "dipping" thickness of 53.9 ± 1.0 nm has been taken from the experiment with the same solution used for testing the influence of potential and time. As the increase in temperature to 41 °C should give a thinner dipping layer, because of the reduced viscosity of the solution, it means that it was probably overestimated. By comparing these results with those reported in Table 1, from which an electrodeposited thickness of about 80 nm is expected with 5-min deposition time, it can be seen that all three the parameters affect the thickness by increasing it significantly.

Chronoamperometry (Fig. 7) suggests that there is a correlation between thickness and current and that oxygen seems to have a greater effect compared to the electrolyte.
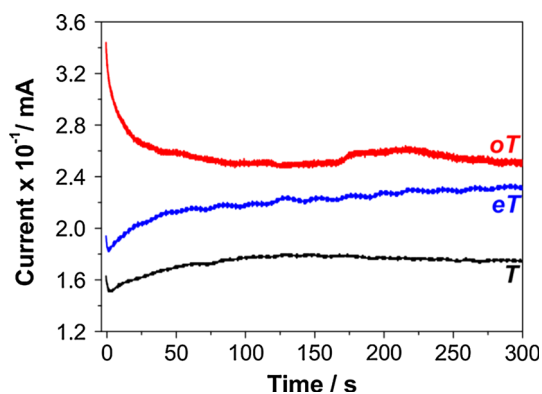
Fig. 7 CA of samples T, eT, oT. Applied potential: -0.9 V versus SCE. Deposition time: 300 s

The CA curves for the samples eT and T show an uncommon behavior, which is still unexplained, but that is quite reproducible.

4 Conclusions

Silica thin films were deposited by the electro-assisted deposition, based on the electrochemical generation of hydroxide ions, with the aim to test different parameters involved in the process. Submicron thicknesses were measured with ellipsometry by using the Cauchy's model.

The influence of potential and time were studied. According to the literature, the thickness grows with the increase in both. Any asymptote with deposition time was not found.

Solutions with different C, R and H ratios were tested, and the thickness was found to increase with both C and H. The effect of R on the thickness could not be checked, as films cracked at $R = 10$.

Temperature seems to be an important factor in the electrodeposition process, from the point of view of thickness, thickness uniformity and integrity of the coating layer.

The presence of oxygen and KNO_3 in solution influences the amount of hydroxide ions at the interface, and thickness was found to increase.

The results obtained in this study are preliminary and need to be supported by further experiments. However, it is

important to underline the fact that a systematic approach was started, with the aim to analyze the factors that make experimentation difficult and to look for possible solutions, thus putting the basis for a more complete and analytic investigation.

References

1. Shacham R, Avnir D, Mandler D (1999) Electrodeposition of methylated sol–gel films on conducting surfaces. Adv Mater 11(5):384–388

2. Shacham R, Mandler D, Avnir D (2004) Electrochemically induced sol–gel deposition of zirconia thin films. Chemistry 10(8):1936–1943

3. Shacham R, Avnir D, Mandler D (2004) Electrodeposition of dye-doped titania thin films. J Sol–Gel Sci Technol 31(1–3):329–334

4. Toledano R, Shacham R (2008) Electrochemical co-deposition of sol–gel/metal thin nanocomposite films. Chem Mater 20(13):4276–4283

5. Toledano R, Mandler D (2010) Electrochemical codeposition of thin gold nanoparticles/sol–gel nanocomposite films. Chem Mater 22(13):3943–3951

6. Farghaly AA, Collinson MM (2014) Electroassisted codeposition of sol–gel derived silica nanocomposite directs the fabrication of coral-like nanostructured porous gold. Langmuir 30(18):5276–5286

7. Sheffer M, Groysman A, Mandler D (2003) Electrodeposition of sol–gel films on Al for corrosion protection. Corros Sci 45(12):2893–2904

8. Sheffer M, Groysman A, Starosvetsky D, Savchenko N, Mandler D (2004) Anion embedded sol–gel films on Al for corrosion protection. Corros Sci 46(12):2975–2985

9. Hu J-M, Liu L, Zhang J-Q, Cao C-N (2006) Effects of electrodeposition potential on the corrosion properties of bis-1,2-[triethoxysilyl] ethane films on aluminum alloy. Electrochim Acta 51(19):3944–3949

10. Liu L, Hu J-M, Zhang J-Q, Cao C-N (2006) Improving the formation and protective properties of silane films by the combined use of electrodeposition and nanoparticles incorporation. Electrochim Acta 52(2):538–545

11. Li M, Yang Y-Q, Liu L, Hu J-M, Zhang J-Q (2010) Electro-assisted preparation of dodecyltrimethoxysilane/TiO2 composite films for corrosion protection of AA2024-T3 (aluminum alloy). Electrochim Acta 55(8):3008–3014

12. Wu L-K, Liu L, Li J, Hu J-M, Zhang J-Q, Cao C-N (2010) Electrodeposition of cerium (III)-modified bis-[triethoxysilylpropyl]tetra-sulphide films on AA2024-T3 (aluminum alloy) for corrosion protection. Surf Coat Technol 204(23):3920–3926

13. Wu L-K, Hu J-M, Zhang J-Q (2012) Electrodeposition of zinc-doped silane films for corrosion protection of mild steels. Corros Sci 59:348–351

14. Jiang L-L, Wu L-K, Hu J-M, Zhang J-Q, Cao C-N (2012) Electrodeposition of protective organosilane films from a thin layer of precursor solution. Corros Sci 60:309–313

15. Wu L-K, Zhang X-F, Hu J-M (2014) Corrosion protection of mild steel by one-step electrodeposition of superhydrophobic silica film. Corros Sci 85:482–487

16. Hu J-M, Liu L, Zhang J-Q, Cao C-N (2007) Electrodeposition of silane films on aluminum alloys for corrosion protection. Prog Org Coat 58(4):265–271

17. Collinson M, Moore N, Deepa P, Kanungo M (2003) Electrodeposition of porous silicate films from ludox colloidal silica. Langmuir 16:7669–7672

18. Maghear A, Etienne M, Tertiş M, Săndulescu R, Walcarius A (2013) Clay-mesoporous silica composite films generated by electro-assisted self-assembly. Electrochim Acta 112:333–341

19. Walcarius A, Sibottier E, Etienne M, Ghanbaja J (2007) Electrochemically assisted self-assembly of mesoporous silica thin films. Nat Mater 6(8):602–608

20. Herzog G, Sibottier E, Etienne M, Walcarius A (2013) Electrochemically assisted self-assembly of ordered and functionalized mesoporous silica films: impact of the electrode geometry and size on film formation and properties. Faraday Discuss 164:259–273

21. Liu L, Toledano R, Danieli T, Zhang J-Q, Hu J-M, Mandler D (2011) Electrochemically patterning sol–gel structures on conducting and insulating surfaces. Chem Commun (Camb) 47(24):6909–6911

22. Deepa P, Kanungo M, Claycomb G, Sherwood PMA, Collinson MM (2003) Electrochemically deposited sol–gel-derived silicate films as a viable alternative in thin-film design. Anal Chem 75:5399–5405

23. Vegliò F (1995) La programmazione della sperimentazione nello sviluppo dei processi chimici. Ratio Math. 9:37–53

24. Leventis N, Chen M (1997) Electrochemically assisted sol–gel process for the synthesis of polysiloxane films incorporating phenothiazine dyes analogous to methylene blue. Structure and ion-transport properties of the films via spectroscopic and electrochemical characterization. Chem Mater 9:2621–2631

25. Lyons MEG (1994) Electroactive polymer electrochemistry. Part 1: fundamentals. Springer US, Boston, 487

26. Mendoza-Huizar LH, Robles J, Palomar-Pardavé M (2003) Nucleation and growth of cobalt onto different substrates Part II. The upd-opd transition onto a gold electrode. J Electroanal Chem 545:39–45

27. Okner R, Favaro G, Radko A, Domb AJ, Mandler D (2010) Electrochemical codeposition of sol–gel films on stainless steel: controlling the chemical and physical coating properties of biomedical implants. Phys Chem Chem Phys 12(46):15265–15273

28. Brinker CJ, Scherer GW (1990) sol–gel science: the physics and chemistry of sol–gel processing. Academic Press Inc, London

29. Collinson MM, Higgins DA, Kommidi R, Campbell-Rance D (2008) Electrodeposited silicate films: importance of supporting electrolyte. Anal Chem 80:651–656

30. Ding S, Liu L, Hu J, Zhang J, Cao C (2008) Nitrate ions as cathodic alkalization promoters for electro-assisted deposition of sol–gel thin films. Scr Mater 59:297–300